UNIVERSIDAD NACIONAL DE COLOMBIA
SEDE MEDELLÍN
FACULTAD DE MINAS

DYNA
http://dyna.medellin.unal.edu.co/

A viable wireless PC assisted alternative to studies of vectorcardiography

Juan Carlos Estrada-Gutiérrez [a], Alfonso Hernández-Sámano [a], Ernesto Edgar Mazón-Valadez [a], José Ávila-Paz [a], Arturo González-Vega [b], Juan Alberto Leyva-Cruz [c] & Mario Eduardo Cano-González *[a]

[a] *Centro Universitario de la Ciénega, Universidad de Guadalajara, Guadalajara, México, jcarlosredes@gmail.com, h.s.alfonso@gmail.com, mazon_valadez@hotmail.com, jocmos@hotmail.com, meduardo2001@hotmail.com*.*
[b] *División de Ciencias e Ingenierías, Universidad de Guanajuato, León, México, ar.glz.ve@gmail.com.*
[c] *Dpto. de Física, Universidade de Estadual de Feira de Santana, Bahía, Brasil, jalbertoleyva@yahoo.com.br.*

Received: February 28th, 2014. Received in revised form: October 28th, 2014. Accepted: November 11th, 2014.

Abstract
The development of an analog device to wirelessly modulate and record twelve cardiac leads, PC assisted is reported. The system, which has been developed using low cost components, contains only one signal conditioning stage and one stage for amplitude modulation with FM transmission/reception. Also it contains an interface to select the cardiac leads remotely, which is based in the transmission/decoding of audible dual frequency tones. The device has been tested on a group of volunteers simultaneously using a registered trademark electrocardiograph, to assess the performance of the new device. Furthermore, the experimental results indicate that the device is a tool suitable to conduct studies of vector-cardiography with maximum uncertainties of 20 % in the cardiac axis orientation measurement.

Keywords: wireless; cardiac; audio; modulation.

Una viable alternativa para estudios de vectorcardiografía de manera inalámbrica asistida por computadora

Resumen
Se presenta el desarrollo de un dispositivo analógico, para modular y registrar de manera inalámbrica las doce derivaciones cardiacas con una PC. El sistema que ha sido desarrollado con componentes de bajo costo, contiene una sola etapa de acondicionamiento de señales, una etapa de modulación de las señales en AM con transmisión/recepción en FM, más un medio de selección de las derivaciones de manera remota, basado en la transmisión/decodificación de tonos audibles de doble frecuencia. El dispositivo ha sido probado en un grupo de voluntarios de manera simultánea empleando un electrocardiógrafo de marca con el fin de evaluar su funcionamiento. Los resultados experimentales indican que el sistema es una herramienta capaz de conducir estudios de vector-cardiografía con una incertidumbre máxima del 20 % en la medición de la orientación del eje cardiaco.

Palabras clave: inalámbrico; cardiaco; audio; modulación.

1. Introduction

The electrocardiographic devices designed to perform diagnostics use 6 electrodes connected on the chest, 3 electrodes on the Einthoven triangle and another one as neutral reference. These electrodes are connected to a stage of conditioning and amplification which allow the detection of signals in the bandwidth from 0.05 to 150 Hz. This is in agreement with the AHA (American Heart Association) to diagnose adolescents and adults [1,2], and with the frequency spectrum of the ECG [3]. Other researchers suggest a bandwidth 0.01 to 100 Hz [4]. These devices are also composed of a cardiac leads selector and a mean for display the electrocardiograms.

Currently are observed several researches about new portables devices to the monitoring of the cardiac beats using smartphones or PC assisted with one or more means of data transmission [5-7]. These kind of interfaces are USB [8], Blue Tooth modules [9], Wi-fi [10] or Zigbee [11]. Other devices possesses a small size and low power consumption [12,13]. Nevertheless, some of these alternatives which work *in situ* or remotely to obtain the

twelve cardiac leads use more than one stage of amplification. This fact increases the cost and volume of the devices. Furthermore, in the last works is not sufficiently explained the stage of selection for the cardiac leads, neither the electrocardiograms presented are compared with others measured simultaneously using a trademark device, in order to qualitatively contrast their working.

In agreement with the AHA, in order to make a more accurate diagnosis of heart function is necessary to measure their activity in a horizontal and vertical plane. Regarding the dipolar-electric approximation to model the heart [14], the electrodes are distributed following different equipotential lines and only 10 electrodes are needed to obtain 12 cardiac leads. Therefore, by analyzing the sense (up or down) of the QRS complex in the derivations D1 and AVF is obtained the quadrant of the axial orientation θ of the cardiac axis. Similarly, analyzing the sense in the precordial V2 we can obtain the sign of the azimuthal orientation φ. The cardiac axis is very important because their variations are related with many cardiac diseases [15]. By analyzing the rate r between the amplitudes R and S from the base line (iso-electric line), is possible to approximate the calculus of θ and φ. For example: if in D1 is observed $r = 1$, the corresponding angle is $\theta = 90°$ with the X axis, therefore the values $r = 1.5$ and 0.5 corresponds with $\theta = 45°$ and $135°$. The sign of θ depends of the sense of R in AVF [15].

Recently our research group has performed a low cost device to convert a bipolar cardiac lead into an audible signal (AM modulated), this signal is transmitted in FM by a transmitter/receiver pair, to be stored trough the audio input of a PC [16]. Although analog transmission could be thought as outdated and has to bear with transmission impairments (Attenuation, Distortion and Noise) as well as the digital transmission does, it flaunts quite a useful characteristic unlike its most modern digital counterpart, the analog transmission inherently bypasses the critical issue of data packet frames losses due to conversion-transmission delays and bottlenecks in the communication protocols which is of utmost importance for the trusty representation of the received signal [17,18]. For this reason the aim of this work is to extend the working of this device by performing the instrumentation to wirelessly obtain the 12 cardiac leads for diagnostic or telemedicine purposes. Moreover, all the measurements are obtained simultaneously with our prototype and a trademark device, which satisfies the standard of the Association for the Advancement of Medical Instrumentation (AAMI). In order to evaluate the working of our new system and their ability to be used in vectorcardiography. Furthermore the device shall require a low cost for their construction using only one stage of conditioning and amplification.

As the measurement of the cardiac leads is carried out differentially, there are two voltage poles V+ and V-, where the first one is more positive with respect to a same neutral reference (connected at the right leg of the patient). Both poles feed an instrumentation operational amplifier.

The Table 1 [15,16,19,20] summarizes the procedure to interconnect the electrodes in order to obtain poles of the 12 cardiac leads using an electronic selector. The notation is: left arm (LA); right arm (RA); left leg (LL); right leg (RL);

Table 1.
Formation of V+ and V- for each cardiac lead.

LEAD	V+	V-
D1	LL	RA
D2	LL	RA
D3	LL	LA
AVR	RA	RA + LL
AVL	RL	RA + LL
AVF	LL	RA + LA
V1	CH1	RA + LL + LA
V2	CH2	RA + LL + LA
V3	CH3	RA + LL + LA
V4	CH4	RA + LL + LA
V5	CH5	RA + LL + LA
V6	CH6	RA + LL + LA

Source: Own

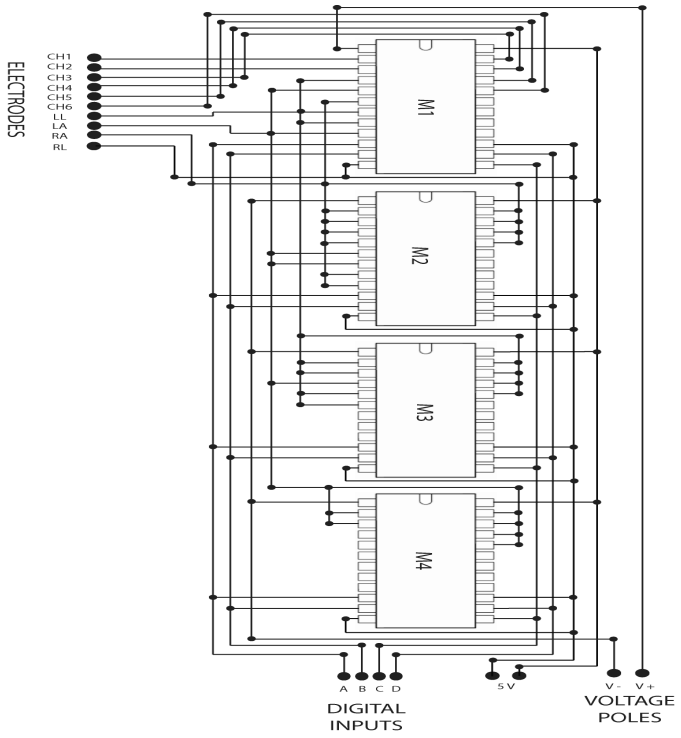

Figure 1. Selector composed of 4 multiplexers to select the voltage poles of each cardiac lead.
Source: Own

fourth intercostal space, just to the right of the sternum (CH1); fourth intercostal space, just to the left of the sternum (CH2); between CH2 and CH4 (CH3); fifth intercostal space in the left mid-clavicular line (CH4); horizontally even with CH4 in the left anterior axilary line (CH5); horizontally even with CH4 and CH5 in the mid-axilary line (CH6); the "+" sign mean electrodes connected.

2. Materials and methods

2.1. Remote selector of the 12 cardiac leads

The cardiac leads selector is performed using an array of 4 analogs multiplexers (HEF4067B) and it is detailed in the Fig. 1. In the bottom the electrodes are connected to

the multiplexers (following the notation of Table 1) whereas on the right side are observed the digital inputs A, B, C, D; also, the output voltage V+ y V- for each cardiac derivation. This kind of multiplexers are characterized for the selection of the 16 possible analog inputs (AI), using a combination of values ABCD. They have a very low total harmonic distortion (THD) and the capability of switching electric current in the range of μA at high speed. Our selector just needs 4 digital inputs in total, which feed at the same time all the multiplexers in order to obtain the pair of voltage poles of any chosen cardiac lead. The Table 2 shows the relationship between the cardiac leads and the digital values ABCD for each multiplexer, also the connections of the electrodes with their analog inputs. This selector is able of generate all the combinations detailed in Table 1.

On the other hand, the values ABCD are obtained using a dual tone decoder, which is designed to decode audible tones of dual frequency (DTMF) HT9170B/D. When this chip receives a dual tone it allows four digital outputs, which could be connected directly to the selector. In the Fig. 2 is shown the diagram of the DTMF, and the Table 3 show the frequencies which compound a tone and their corresponding digital outputs, for each digit employed.

Table 2.
Multiplexer Performance Summary.

Lead	DGTL. V.				M1		M2		M3		M4	
	D	C	B	A	AI	E	AI	E	AI	E	AI	E
D1	0	0	0	0	0	LA	0	RA	0	NC*	0	NC
D2	0	0	0	1	1	LL	1	RA	1	NC	1	NC
D3	0	0	1	0	2	LL	2	LA	2	NC	2	NC
AVR	0	0	1	1	3	RA	3	LA	3	LL	3	NC
AVL	0	1	0	0	4	LA	4	RA	4	LL	4	NC
AVF	0	1	0	1	5	LL	5	RA	5	LA	5	NC
V1	0	1	1	0	6	CH1	6	RA	6	LL	6	LA
V2	0	1	1	1	7	CH2	7	RA	7	LL	7	LA
V3	1	0	0	0	8	CH3	8	RA	8	LL	8	LA
V4	1	0	0	1	9	CH4	9	RA	9	LL	9	LA
V5	1	0	1	0	10	CH5	10	RA	10	LL	10	LA
V6	1	0	1	1	11	CH6	11	RA	11	LL	11	LA

*NC: Not Connect.
Source: Own

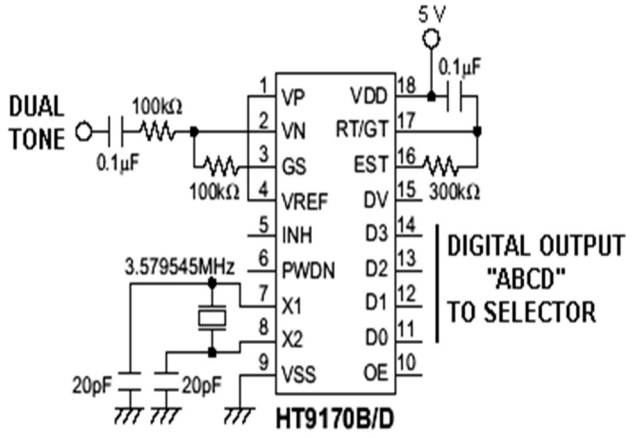

Figure 2. Diagram of the tone decoder DTMF.
Source: Own

Table 3.
Frequencies corresponding to each DTMF and their respective decoded digital value.

Low Frequency	High Frequency	Digit	D	C	B	A
697	1209	1	0	0	0	1
697	1336	2	0	0	1	0
697	1477	3	0	0	1	1
770	1209	4	0	1	0	0
770	1336	5	0	1	0	1
770	1477	6	0	1	1	0
852	1209	7	0	1	1	1
852	1336	8	1	0	0	0
852	1477	9	1	0	0	1
941	1336	0	1	0	1	0
941	1209	*	1	0	1	1
941	1633	D	0	0	0	0

Source: Own

The DTMF of Table 3, are superimposed sine waves and correspond to the sound heard when the digit of some telephonic devices is pressed. For instance: when a sinusoidal pulse composed of 697 Hz and 1209 Hz signal is received (corresponding to the digit 1), their correct decoding allow us the 4 digital values 0001, which, in accord with Table 2 correspond to the D2 lead. In our design, the tones corresponding to each digit are generated from a computer via the audio output, with maximum amplitude of 300 mV. This switching interface can operate in full wired way, nevertheless it is very easy to adapt to the digital outputs of a microcontroller to other applications. However, since the goal is to work wirelessly, the tones are transmitted using an FM audio-transmitter (ideal for microphone). To demodulate the FM signal, the tone must be amplified up to a value close to 1 V, therefore the FM receiver is connected to a non-inverting amplification stage using an operational amplifier with gain $G = 11$, in order to feed the DTMF and avoid decoding errors.

In summary, the procedure for remotely selection of a cardiac lead is the following: at first, from the PC audio output, the dual tone are generated and transmitted as FM, the receiver output is amplified and introduced to the DTMF which generate the four digital signals to feed the lead selector, where the two poles that feed the amplifier are obtained, the output is then modulated in amplitude and transmitted by a second FM transmitter, to then be acquired through the audio card and digitally demodulated on a PC.

2.2 Heart signal amplifier and conditioner

A schematic diagram of the full system is shown in the Fig. 3(A), where it can see the electrodes on the patient and connected to the selector, which feeds the instrumentation amplifier, connected to the AM modulator and then to the (FM2) transmitter. Also the DTMF connected to the multiplexer and to the receiver of the (FM1) transmitter are displayed. In the same way, it can be observed the audio card output of a laptop connected to the FM1 to transmit the tone, and the FM2 receiver connected to the audio card input, where the AM signals are demodulated. While the Fig. 3(B) shows the corresponding block diagram. To avoid potential interference, care should be taken that the FM1 modulation frequency is not an integer multiple of FM2.

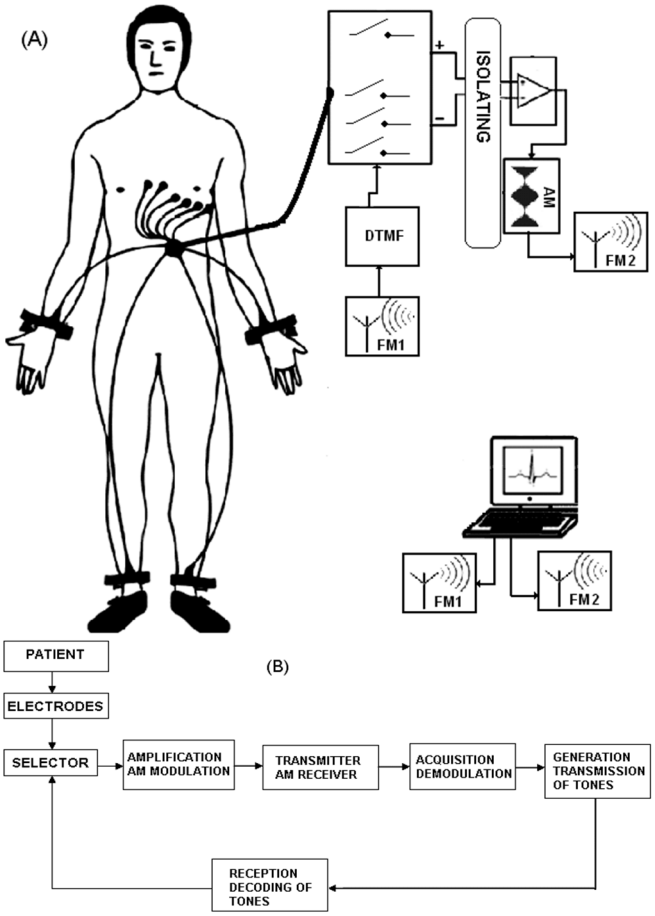

Figure 3. (A) Schematic diagram of the system and (B) block diagram respectively.
Source: Own

The amplification consists of six stages built with mostly inexpensive electronic components. As shown in Fig. 4, the first stage is used to increase the CMRR of the instrumentation amplifier and is connected to the right leg of the patient, then is used an AD620 instrumentation amplifier with gain given by eq. (1).

$$G_1 = \frac{49.4k\Omega}{R_{G1}} + 1 = 4.29 \quad (1)$$

which is feedback to the reference input by means of an operational amplifier on integrating configuration, with this step, the base line signal is stabilized, since it has a high pass filter behavior. Then there is a non-inverting amplifier stage with gain given by eq. (2).

$$G_2 = \frac{R_{G2}}{R1} + 1 = 5.7 \quad (2)$$

followed by a rejection stage for the 60 Hz frequency and an active four order butterwort type low pass filter with gain G_3 = 4; and finally a last non-inverting amplification with a gain G_4 = 2, plus the option to regulating the DC level to take control of the voltage levels that will be modulated in amplitude. Except for the feedback stage, rejection of 60 Hz and stabilization of the baseline stage, all other steps are explained in [16]. With this amplifier and selector it is achieved: A bandwidth of 0.034 to 150 Hz with a signal/noise ratio about to 40 dB, total gain G_t = 195.62, input impedance of 1 GΩ (according to the datasheet for the AD620), common mode rejection CMRR close to 100 dB since all the used amplifiers have a CMRR of about 110 dB, restoration time for base line minor than 3 s and adjustable DC level. Prior to the differential amplification stage, each electrode are connected to a voltage follower using an operational amplifier for the correct coupling of the electrodes and the subsequent circuits (See dotted line in Fig. 4). At the output of each follower a 47 kΩ resistor are connected to decrease any potential leakage currents and clipping diodes that discharge overvoltage to the power supply. The leakage currents sensed between terminals (lead-lead) and between terminals and ground (lead-ground) are less than 10 μA (in good agreement with [20,21]). Additionally, to avoid exposing patients to possible variations of the line voltage, the device is powered by a 12v battery connected to a regulating circuit for a dual voltage output of ± 5 V.

In the graphs of Fig. 5, are displayed two curves experimentally determined (T1 y T2). The one of a Fukuda Denshi Cardimax FX-1201 electrocardiograph used as reference pattern (T1) and the signal obtained from our new device (T2), respectively. In this experiment the curves are obtained using a function generator Stanford Research mod. DS335 and an oscilloscope Tektronix DPO7104. It is observed that the curve obtained with the reference device T1 has a minimum cutoff frequency 0.05 Hz followed by a rejection of the 60 Hz band with an attenuation of -30 dB and a maximum cutoff frequency of 100 Hz. Whereas T2 has a minimum cutoff frequency of 0.034 Hz, then a rejection to the 60 Hz frequency of -19 dB and a maximum cutoff frequency of 150 Hz. Our observations indicate that increasing the attenuation of the 60 Hz signal with the notch filter lead to a reduction of components of the signals which may be important for a possible diagnostic, for instance: between the range of 30 a 40 Hz [3]. It is also noted that for T1 the attenuation is higher than in T2 for frequencies between 80 Hz and 100 Hz. Even so frequencies between 100 Hz and 110 Hz have a slightly higher intensity than all other (around 0.8dB), due to the established gain in the low-pass and to its transfer function [22].

2.3. Amplitude modulator of the cardiac leads

To the AM modulation an integrated circuit of the family MC1496BPG specially designed this purpose is employed. This circuit provides a lower total harmonic distortion (THD) than the modulation method based on a simple arrangement of differential transistors as used in [16], while the 2 kHz carrier signal is generated with a double integrator arrangement based on an operational amplifier as in [16]. The Fig. 6 shows the electronic circuit diagram of the modulator. Once the amplitude is modulated,

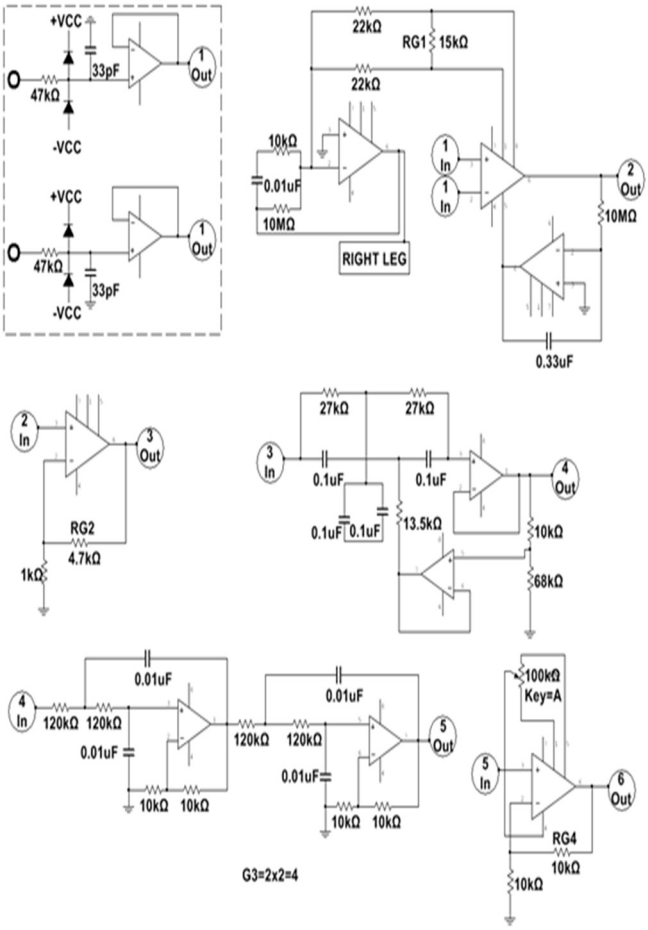

Figure 4. Amplifier and conditioner circuit for the cardiac leads.
Source: Own

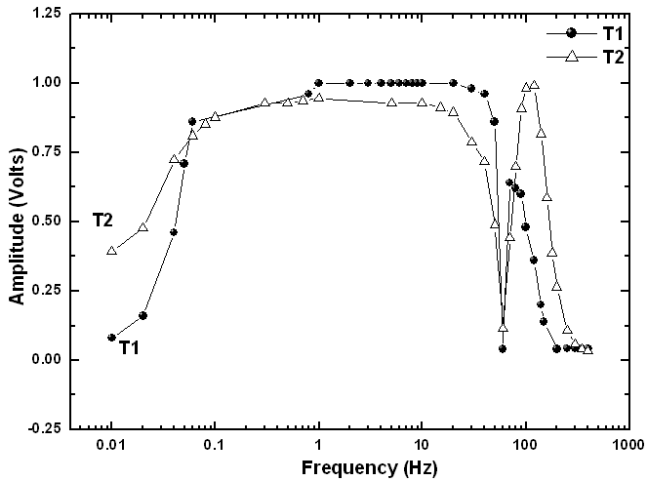

Figure 5. Experimental curves T1 (reference device) and T2 (AM modulator) of the frequency response of both devices.
Source: Own

the cardiac signal is converted into audible signal which are transmitted using a commercial microphone FM transmitter-

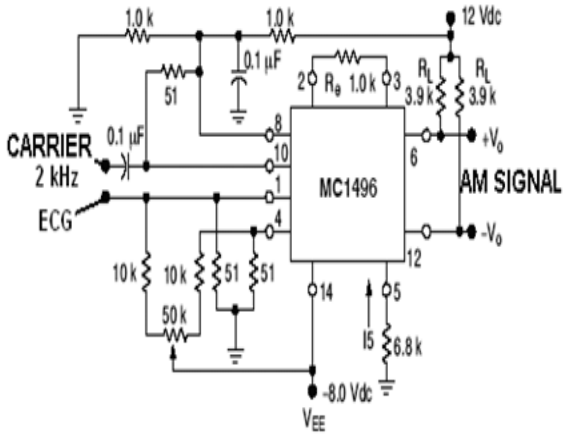

Figure 6. AM modulator circuit diagram of the cardiac signal.
Source: Own

receiver system. The acquisition of the "audible cardiac signals" is performed using the audio input of a PC with a maximum sampling capacity of 192000 kS/s, 16 bits resolution, THD lower than 0.1% and bandwidth from 4 Hz to18 kHz in the Lab-View 8.2 environment. A similar setup is realized in [23]

2.4. Demodulation of the amplitude modulated leads

For the signals demodulation, the National Instruments demodulation toolkit is used. As the cardiac signals of each person may vary in amplitude, moreover the amplitudes of the precordial signals are usually greater than the bipolar leads in the same subject, then the modulation factor of each measure lead changes considerably which could cause changes to the original signal, if is not properly demodulated. However, in this work a coherent type AM digital demodulation is used, which takes the carrier signal as an input parameter and it is independent of the modulation factor, as is described in below.

Initially the envelope signal *m(t)* becomes the signal described in eq. (3).

$$x(t) = (C + m(t))\cos(wt) \tag{3}$$

where *C* is a constant that depends on the amplitude of the carrier signal. Multiplying the eq. (3) by *cos(wt)* and using the trigonometric identity $cos^2(\theta) = ½ + cos(2\theta)/2$ is obtained the eq. (4)

$$y(t) = (C + m(t))\left(\frac{1}{2} + \frac{1}{2}\cos(2wt)\right) \tag{4}$$

Subsequently, to recover the *m(t)* signal, the *y(t)* signal is filtered using a band-pass filter tuned to the frequency *w,* in order to remove the DC component and higher frequencies than the carrier signal. Finally the result is multiplied by 2.

3. Measurements and discussion

3.1. Measurements of 12 leads modulated

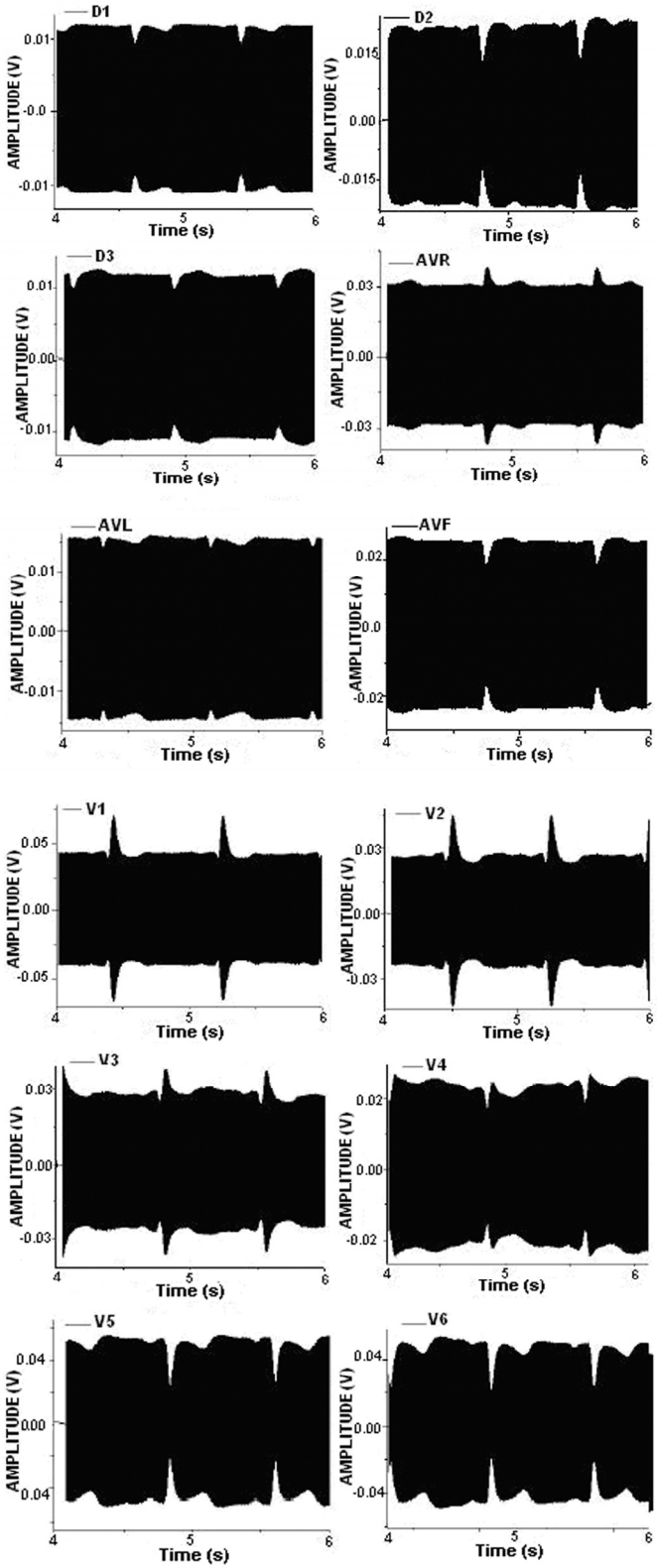

Figure 7. Graphs of the 12 modulated leads using a commercial ecg simulator.
Source: Own

After all the design, simulation and assembly work of the electronic device, the execution stage of experiments began, in order to test the ability of detection and acquisition using a commercial ecg signal simulator. In the Fig. 7 is show a typical measurement of the 12-lead amplitude-modulated. By analyzing the graphs, are evidenced higher modulation factors in the precordial leads. In these measurements the maximum THD observed oscillates around 4%, this is due to nonlinear behavior of the semiconductor components of the transmission/reception of signals system. However, the demodulated signals shows THD values lowers than 1% due to the lowpass filter of high order implicit in the digital demodulate method.

3.2. Measurements with volunteers

Thereafter, measurements of 12 cardiac leads (intervals of 3 seconds per lead) are obtained from a group of 12 volunteers with no history of heart disease, as follows: the electrodes are connected to our device and simultaneously to the inputs of the electrocardiograph of reference ECG_{ref}. The signals of ECG_{ref} are acquired of wired manner from a laptop over a distance of *10 m*, using an analog acquisition interface USB-6805 from National Instruments, with 5 kS/s of sampling frequency and a shielded USB cable. While the same cardiac lead is modulated in AM and transmitted by

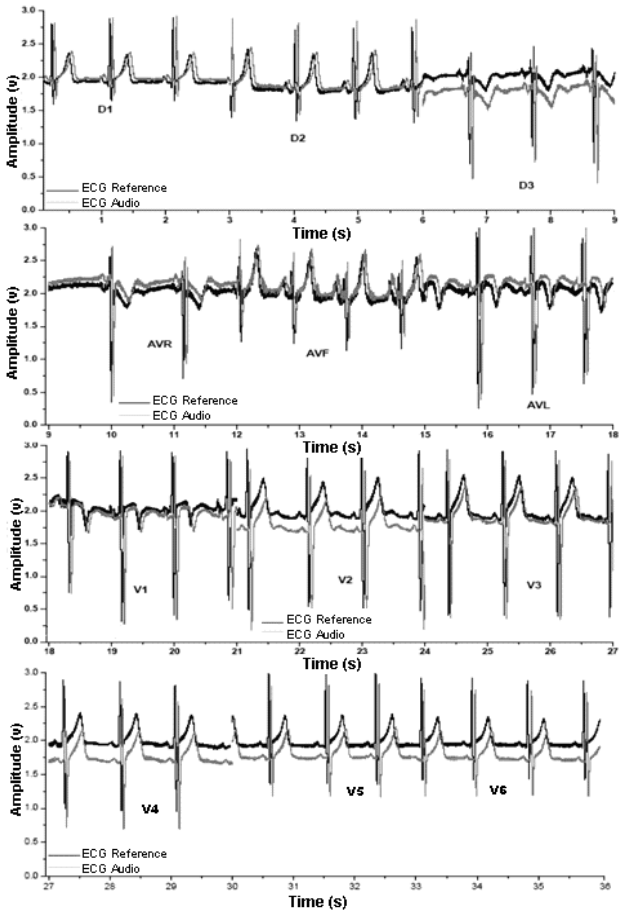

Figure 8. Graphs of the demodulated 12 leads of a volunteer (gray line) and those obtained simultaneously with the reference device (black line).
Source: Own

FM2 (trademark ROMMS mod. MC-100), to the audio input of the same computer. The data are acquired with sampling frequency of 50 kS/s, in order to demodulate, store and graph them in real time; on a same graphical interface developed in LabView environment. Each lead is selected wirelessly from the same distance (10 m) using the FM1 transmitter (trademark steren, mod. Mic-280).

In the Fig. 8 is shown the measurements of the 12 leads of the same volunteer, using both devices. Plotting the measured signals by the two methods is generally observed a shift in the amplitude and time. This observed displacement in the amplitudes can be explained by the different DC levels (offset) found in the signals. Furthermore the horizontal shift is due to the period to the acquisition, digitization, demodulation and sampling. Moreover, in Fig. 9 are displayed the ECG signals of D1 acquired with both devices, they are shown overlapped deliberately, in order to visibly compare the measurements more clearly. As can be observed the shape of the undulations, intervals and segments which compound the signals are maintained. This fact is very important because the iso-electric lines and amplitudes using both devices must be conserved, in order to carry out a correct determination of θ and φ. Nevertheless, a further analysis is also necessary.

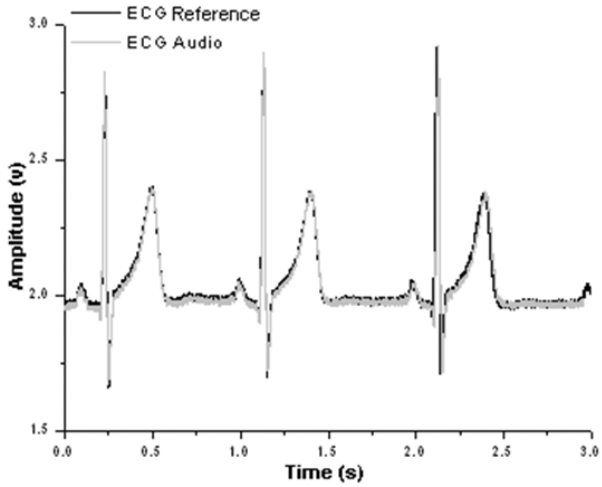

Figure 9. Overlapped graphs of D1, simultaneously taken with the audio input (gray line) and with the pattern device (black line).
Source: Own

3.3. Quantitative comparison between both devices

Actually there are several investigations [15,24-27], which employee different alternatives to the comparison of two signals. They are based in the direct measurement of the parameters of cardiology, or by calculating those parameters using signal processing based on Wavelets.

For this purpose, initially we have done a subroutine in the Labview acquisition program to set the base lines (offset) at the same level and subtract the time shifting between them, in order to start at the same point. Likewise the acquired signals through the USB-6508 card are interpolated to match the number of samples acquired via the audio input. In this way are evaluated the absolute relative deviations (ARD) between the two signals point to point, following the definition of the eq. (5). In the graph of the Fig. 10(A) it can see the typical values of ARD of the volunteer 12 leads, whereas the Fig. 10(B) shows the typical values of ARD of the V2 lead, where are displayed the deviations to the amplitudes of the complex P, QRS and T. After a careful analysis of the ARD values in the leads of each volunteer, it is observed that the largest differences occur in the peak values of the QRS (mainly those associated with the amplitudes of the R and S), becoming more evident in leads of higher amplitude as V2, V4 and V5 and reaching differences up to 15 %.

To determine the differences between the lengths L of the main intervals or segments of both kind of signals, the graph of D1 was analyzed in Origin 6.0 (the leads D1 or D2 are normally used for the reference device) of each volunteers, using the peak detection tool (peak detection). Next, the average value of the ARD is calculated following eq. (6) and the percentage values obtained are shown in the second row of Table 4. The same criterion is employed to determine the AARD values of the undulations P, Q, R, S and T, in the lead D2 as is shown in the last row of Table 4.

$$ARD_{\text{Re}\,ference/\,Audio} = \frac{\left\langle A_{\text{Re}\,ference}\right\rangle - \left\langle A_{Audio}\right\rangle}{\left\langle A_{\text{Re}\,ference}\right\rangle} \qquad (5)$$

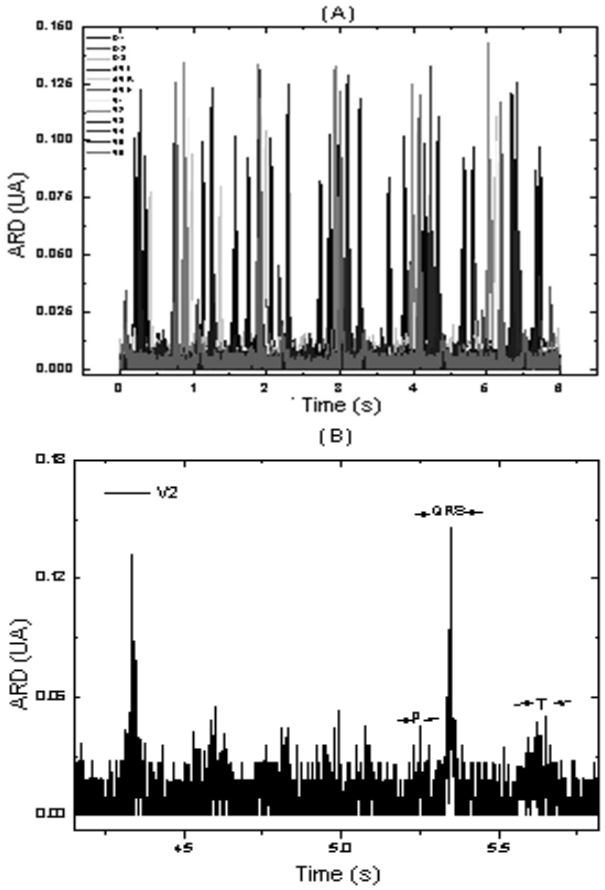

Figure 10. (A) Typical values of ARD (dimensionless) obtained in the 12 leads and (B) of V2 lead with, deviations related to the amplitudes of the complex P, QRS and T.
Source: Own

Table 4.
Percentage values of ARD between the lengths L of the main intervals or segments of the D1 lead

ECG	*ST seg.* %	*PR seg.* %	*PR int.* %	*QRS int.* %	*QT int.* %
AARD	7	5	7	7	9
ECG	*Pamp.* %	*Qamp.* %	*Ramp.* %	*Samp.* %	*Tamp.* %
AARD	4	4	10	8	6

Source: Own

$$AARD_{\text{Re}\,ference/\,Audio} = \frac{1}{N}\sum_{i=1}^{N}\left(\frac{\left\langle L_{\text{Re}\,ference}\right\rangle - \left\langle L_{Audio}\right\rangle}{\left\langle L_{\text{Re}\,ference}\right\rangle}\right)_i \quad (6)$$

These ARD and AARD values experimentally found in the interval and segments of the signals, may be due to small variatios of the carrier AM signal, wereas the AARD values of the amplitudes are due to the differences in the frequency response of both devices, as shown in Fig. 5. Indeed, analyzing the *AARD* values of *Ramp.* and *Samp.* of the Table 4 and regarding that the cardiac axis is related with the ratio of the amplitudes $r = R/S$, the maximum expected error of cardiac axis orientation (eq. (7)) could be close to 20 %. This finding shows the importance of comparing all the alternatives of electrocardiographic devices, against a pattern device, for example [5-13].

$$r_{\max imum} = \frac{R + AARD(Ramp)}{S - AARD(Samp)} \quad (7)$$

4. Conclusions

In this work is presented in detail a low cost viable alternative PC assisted to determine 12-lead electrocardiograms (one by one), using a single stage of amplification and filtering, to conduct studies of vector-cardiography. The leads can be selected and stored using the audio input and output of a computer respectively; and a pair of inexpensive audio transmitter/receiver devices.

Using an AM modulator with audible carrier, each lead becomes an audio signal, and could be transmitted through the microphone input of an economic mobile phone device. In the same way, using the telephone keypad and headphone output the desired cardiac lead can be selected. Nevertheless the module of analog transmission/reception can be easily replaced by a modern digital transmission system, in order to obtain the twelve cardiac leads through a peripheral port, like USB or COM.

We have developed an alternative to the selection of cardiac leads using an arrangement of commercial analog multiplexers, which can be controlled wired or wirelessly from the audio output of a PC, using dual frequency tones and a tone decoder. However, the selector can be used to easily switch between cardiac leads via digital outputs from another device such as: a parallel port, a microcontroller, a digital signal transmitter zigbee or manually using a 4-digit keypad. So that, many devices reported for evaluation the vertical plane of the heart, could be extended by adapting this selector in order to perform studies of vectorcardiography and the criterions of eq. (7) to evaluate the viability of the devices could be used.

The system can be reproduced by an approximate cost of US$90 and exhibits a good performance according to the trademark pattern device, which meets the international standards for electrocardiography. Therefore it shown to be a viable tool to measure cardiac bio-electric potential, for telemedicine applications [28], research in biomedical engineering or in teaching activities. Due to their low cost, the device represents a suitable tool to be used in developing countries, similar to [29].

Acknowledgements

The authors wish to thank the facilities provided for obtaining measurements to the staff of the regional hospital of the IMSS in Ocotlán Jalisco and to CONACyT by the support given to students.

References

[1] Kligfield, P., Gettes, L.S., Bailey, J.J., Childers, R., Deal, B.J., Hancock, E.W. et al. Recommendations for the standardization and interpretation of the electrocardiogram: Part I: The electrocardiogram and its technology: A scientific statement from the American Heart Association Electrocardiography and Arrhythmias Committee, Council on Clinical Cardiology; the American College of Cardiology Foundation; and the Heart Rhythm Society. Endorsed by the International Society for Computerized Electrocardiology. Heart Rhythm, 4 (3), pp. 394-412, 2007. http://dx.doi.org/10.1016/j.jacc.2007.01.024

[2] Pipberger, H.V. et al., Recommendations for standardization of leads and specifications for instruments in electrocardiography and vector cardiography. Circulation, 52, pp. 11-31, 1975.

[3] Ferrero, C.A. and Hall, E.J., Textbook of Medical Physiology, 11 ed., Mc Graw-Hill, Spain, 2001. pp. 103-114,

[4] Henneberg, K.A., Biopotentials and electrophysiology measurement, in Aller Mauren. Measurements instrumentation and sensors Handbook, CRC press, 2a ed., Boca Raton, Florida, 1999, pp. 2019-2037.

[5] Silva, C.V. and Rojas, V.G., Design and implementation of a digital electrocardiographic system Rev.Fac.Ing.Univ. Antioquia, 55, pp. 99-107, 2010. Available at: http://jaibana.udea.edu.co/grupos/revista/revistas/nro055/Articulo%2010.pdf

[6] Tseng Y-L., Shi Y.-Z., Jaw F.-S., Portable, real-time, 12-lead ecg monitoring system, Instrumentation Science & Technology, 38 (4), pp. 305-312, 2010. http://dx.doi.org/10.1080/10739149.2010.508331

[7] Najeb, J.M., Ruhullah, A. and Sh-Hussain, S., 12-Channel USB data acquisition system For QT dispersion analysis, Proceedings of the International Conference on Robotics. Vision, Information and Signal Processing ROVISP, pp. 83-86, 2005. Available at: http://eprints.utm.my/2151/1/Najeb_ROVISP_2005.pdf

[8] Lucani, D., A portable ECG monitoring device with Bluetooth and Holter capabilities for telemedicine applications. Proceedings of the 28th IEEE EMBS Annual International Conference New York City, USA, pp. 5244-5247, 2006. http://dx.doi.org/10.1109/IEMBS.2006.260798

[9] Jia-Ren, C.C. and Cheng-Chi T. A new wireless-type physiological signal measuring system using a PDA and the Bluetooth technology, Instrumentation Science & Technology, 37 (5), pp. 503-515, 2009.

[10] Nopparat, V., The three-lead wireless ECG in sensor networks for mobile patients. SICE Annual Conference, pp. 2308-2311, 2008. http://dx.doi.org/10.1109/SICE.2008.4655050

[11] Auteri, V., Roffia, L., Lamberti, C. and Cinotti, T.S., Zigbee-based Wireless ECG Monitor, Computers in Cardiology, 34, pp. 133-136, 2007. http://dx.doi.org/10.1109/CIC.2007.4745439
[12] Thaddeus, R.F., Fulford-Jones, G-Y.W., and Welsh, M., A Portable, Low-Power, Wireless Two-Lead EKG System. In Proceedings of the 26th Annual International Conference of the IEEE EMBS San Francisco, CA, USA, pp. 2141-2144, 2004. http://dx.doi.org/10.1109/IEMBS.2004.1403627
[13] Borromeo, S., Rodriguez-Sanchez, C., Machado, F., Hernandez-Tamames, J.A. and de la Prieta, R.A., Reconfigurable, wearable, wireless ECG system. In Proceedings of the 29th Annual International Conference of the IEEE EMBS Cité Internationale, Lyon, France, pp. 1659-1662, 2007. http://dx.doi.org/10.1109/IEMBS.2007.4352626
[14] Gabor, D. and Nelson, C.V., Determination of the resultant dipole of the heart from measurements on the body surface, Journal of Applied Physics, 25, pp. 413-416, 1954. http://dx.doi.org/10.1063/1.1721655
[15] Davis, D., Quick and Accurate 12-Lead ECG Interpretation 4a ed., Philadelphia, USA, Lippincott Williams & Wilkins, 2007, pp. 6-7. Available at: http://resourcecenter.ovid.com/site/catalog/Book/4961.pdf
[16] Cano, M.E., Jaso, R.A., Tavares, R.A., Estrada, J.C., Mena, E.A., Reynoso, O., González, V.A. and Córdova, T. A simple alternative for modulating and recording the PQRST complex. Rev. Mex. de Ing. Biomédica, 31 (2), pp. 100-108, 2011. Available at: http://www.medigraphic.com/pdfs/inge/ib-2011/ib112f.pdf
[17] Chiuso, A., Laurenti, L. and chenato, A.Z., LQG cheap control subject to packet loss and SNR limitations. 2013 European Control Conference (ECC), Zürich, Switzerland, 2013. Available at: http://ieeexplore.ieee.org/stamp/stamp.jsp?tp=&arnumber=6669629
[18] Elia, N., Remote stabilization over fading channels, Systems and Control Letters, 54, pp. 237-249, 2005. http://dx.doi.org/10.1016/j.sysconle.2004.08.009
[19] Guyton, C.A., John, H.E., Textbook of Medical Physiology. 11va. ed., Spain, Mc Graw-Hill, 2001. pp. 103-114.
[20] Association for the Advancement of Medical Instrumentation, Cardiac monitors, heart rate meters and alarms. ANSI/AAMI EC13–1992. Arlington (VA): AAMI, American National Standard. 2002. Available at: http://www.pauljbennett.com/pbennett/work/ec13/ec13.pdf
[21] Association for the Advancement of Medical Instrumentation, American National Standard Safe Current Limits for Electromedical Apparatus, ANSI/AAMI ES1-1993. Arlington (VA): AAMI, American National Standard. 1993. Available at: https://courses.engr.illinois.edu/ece445/documents/Safe_Current_Limits.pdf
[22] Ying-Wen B., Chien-Yung C., Cheng-Kai L., Chuang-Hsiang H., Yuh-Ting Ch. and Ya-Nan L. Adjustable 60Hz Noise Reduction and ECG signal amplification of a remote electrocardiogram system. In proceedings of the Instrumentation and Measurement Technology Conference Vail, CO, USA, pp. 197-202, 2003. Available at: http://cs.ee.fju.edu.tw/paper/200301.pdf
[23] Stojanovic, R. and Karadaglic, D., An economical and feasible teaching tool for biomedical education Computer-Based Medical Systems (CBMS), 2011 24th International Symposium on, 1, pp. 1-5, 2011. http://dx.doi.org/10.1109/CBMS.2011.5999116
[24] Dubin, D., Rapid Interpretation of EKG's. 6ta ed. Tampa,FL, Cover Pub Co, pp. 75-76, 2000.
[25] Olarte, O.J., Sierra, D.A. and Rueda, O.L., System for the recognition and diagnostics of cardiac arrhythmias applied to the identification of wide complex tachycardia from the ECG. Rev. Fac. Ing. Univ. Antioquia, 48, pp. 153-164, 2009. Available at: http://ingenieria.udea.edu.co/grupos/revista/revistas/nro048/48-15.pdf?origin=publication_detail
[26] Sivannarayana, N. and Reddy, D.C., Biorthogonal wavelet transforms for ECG parameters estimation. Medical Engineering and Physics, 21, pp. 167-174, 1999. http://dx.doi.org/10.1016/S1350-4533(99)00040-5
[27] Dumont, J., Hernández, A.I. and Carrault, G., Parameter optimization of a wavelet-based electrocardiogram delineator with an evolutionary algorithm. Computers Cardiology, 32, pp. 707-710, 2005. http://dx.doi.org/10.1109/CIC.2005.1588202
[28] Castellano, N.N., Gázquez, J.A., López, J.F. and Manzano, F., Telemetry system for transmission data from an ambulance. DYNA, 79 (175), pp. 43-51, 2012. Available at: http://www.scielo.org.co/pdf/dyna/v79n175/v79n175a05.pdf
[29] Walker, B.A., Khandoker, A.H. and Black, J., Low cost ECG monitor for developing countries. Intelligent Sensors, Sensor Networks and Information Processing (ISSNIP), 2009 5th International Conference on 7 - 10 Dec. 2009 Melbourne, VIC, pp. 195-199, 2009. http://dx.doi.org/10.1109/ISSNIP.2009.5416759

J.C. Estrada-Gutiérrez, received the PhD. degree in Sc. in 2014 from the Universidad of Guadalajara, México, Full Professor en the Technologic Sciences department in the Centro Universitario de la Ciénega of the Universidad de Guadalajara, in México. His research interest include: Magnetic Hyperthermia, Automation and Control and Embedded Systems.

A. Hernández-Sámano, received the MPhys. degree in 2013 from the University of Guanajuato, México, he is Student in the PhD in physics in the Centro Universitario de la Ciénega of the Universidad de Guadalajara, in México. His research interest include: Magnetic Hyperthermia, Resonant Inverters and Magnetometry.

E.E. Mazón-Valadez, received, the BIE. degree in 2012 from the Universidad of Guadalajara, México, he is Student in the Masters in physics in the Centro Universitario de la Ciénega of the Universidad de Guadalajara, in México. His research interest include: Magnetic Hyperthermia, Resonant Inverters and SAR.

J. Ávila-Paz, received MSc.in 2003 from the Universidad Central Marta Abreu de las Villas, Cuba, Full Professor in the Technologic Sciences department in the Centro Universitario de la Ciénega of the Universidad de Guadalajara, in México. His research interest include: Magnetic Hyperthermia, Automation and Control, and Embedded Systems.

A. González-Vega, received the PhD degree in Ciences in 2007 from the Centro de Investigación en Matemáticas A.C. Mexíco. Full professor in the Biomedical Engineering department in the División de Ciencias e Ingenierías de la Universidad de Guanajuato, in México. His research interest include: Biomechanics, biomaterials, optics process, instrumentation and signal and image processing.

J.A. Leyva-Cruz, received the PhD degree in Ciences in 2005 from the Universidade de São Paulo, Brazil. Full professor in the Physics Department in the Universidade Estadual de Feira de Santana (UEFS) na Bahia, in Brazil. His research interest include: Bioinstrumentation, electric and magnetic imaging in medicine, acquisition and automatic processing of biosignals, inverse problems and photoconductive sensors.

M.E. Cano-González, received the PhD degree in Physics in 2007 from the University of Guanajuato, México. Full professor in the Basic Sciences department in the Centro Universitario de la Ciénega of the Universidad de Guadalajara, in México. His research interest include: Magnetic Hyperthermia, Resonant Inverters and Monte Carlo Simulations.